

Influence of non-axisymmetric magnetic perturbations on the equilibrium reconstruction at ASDEX Upgrade

J. C. Fuchs¹, T. Eich¹, R. Fischer¹, L. Giannone¹, A. Herrmann¹, B. Kurzan¹, P. de Maré¹,
P. J. McCarthy², J. Neuhauser¹, W. Suttrop¹, W. Schneider¹, E. Wolftrum¹,
and the ASDEX Upgrade Team¹

¹Max-Planck-Institut für Plasmaphysik, EURATOM Association, Garching, Germany

²Department of Physics, University College Cork, Ireland.

1. Introduction

At ASDEX Upgrade eight in-vessel saddle coils have been recently installed, four coils toroidally spaced at the low field side above the mid-plane and four coils below the midplane. Non-axisymmetric magnetic perturbations produced by these saddle coils have successfully been used to mitigate the plasma energy loss and peak divertor power load linked to Edge Localized Modes (ELMs), whereas concerning confinement, plasma density and impurity concentration both unperturbed ELMy reference discharges and plasmas with mitigated ELMs show a similar behavior [1].

The main tool for equilibrium reconstruction at ASDEX Upgrade is the CLISTE interpretative code [2] which numerically solves the Grad-Shafranov equation as a best fit to a set of experimental measurements, especially from magnetic probes and flux loops. Since the Grad-Shafranov equation assumes toroidal symmetry of the plasma, any effects of the non-axisymmetric magnetic perturbations of the new saddle coils on the equilibrium is not taken into account. In this paper the influence of the magnetic field from the saddle coils on the equilibrium reconstruction is investigated. Possible consequences are discussed, in particular inconsistencies of the mapping of measurements from several diagnostics in different toroidal positions onto flux surfaces, especially at the pedestal, or other effects like strike point splitting, which is observed in the thermographic measurements.

2. Influence of the saddle coils on magnetic probe measurements

The mutual inductance of the saddle coils and the magnetic probes has been used to correct the measurements of the magnetic probes, which are all located at the same toroidal position. It turns out that the influence of the magnetic field from the saddle coils on the magnetic probe measurements is negligible for most probes and reaches corrections of 1-2% only for

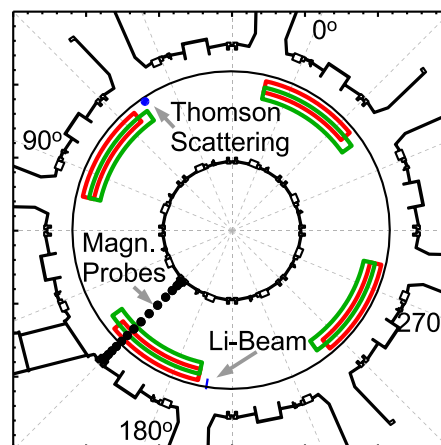


Fig. 1: Toroidal view of ASDEX with the position of the saddle coils (red: upper, green: lower) and of some diagnostics used in this paper: black: magnetic probes, blue: Thomson scattering and lithium beam

those probes which are located near the coils. Correspondingly, when using these corrected probe measurements for the equilibrium reconstruction, assuming toroidal symmetry, almost no effect of the saddle coils on the reconstructed equilibrium can be seen. Only at the low field side near the saddle coils the reconstructed separatrix position is shifted by less than 1 mm. This value is within the error bars of the reconstruction and clearly less than e.g. the shift of the separatrix caused by ELMs which is several mm.

3. Threedimensional perturbation of the equilibrium

However, the equilibrium reconstruction by CLISTE is done under the assumption of toroidal symmetry, and any non-axisymmetric effects are not taken into account. In order to get an estimate how the ideal magnetic field structure is perturbed by the field of the saddle coils, field lines have been followed by a three dimensional field line tracing code, where the total magnetic field was assumed to be the sum of the magnetic field from the unperturbed equilibrium and the vacuum field of the saddle coils which has been calculated previously using Bio-Savart's law [3]. The shielding of the perturbation field by the plasma has been neglected in these calculations.

A series of identical discharges with 1MA plasma current, a toroidal magnetic field of -2.4 T, fractional Greenwald density of $n_e/n_{GW} \sim 0.64$, 9.7MW additional heating and 1kA saddle coil current has been performed, where only the configuration of the saddle coils has been varied: 2 discharges with mode number $n=2$, odd up/down-parity (i.e. opposite polarity of upper and lower coils at the same toroidal position), with zero and 90 degrees toroidal orientation of the magnetic perturbations, and one discharge with $n=2$, even parity.

Figure 2 shows a result of the field line tracing calculations for the first of these discharges ($n=2$, odd parity). Plotted are the connection lengths to the low field side target from field lines starting at a horizontal plane at the height of the lithium beam diagnostic ($z=0.326$ m)

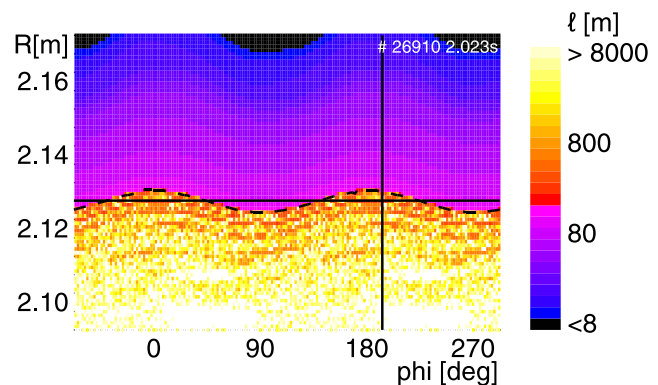


Fig. 2: Connection length to the low field side target for field lines starting at a horizontal plane at $z=0.326$ m (height of the lithium beam) around the torus. Marked are the position of the lithium beam at $\phi=193^\circ$ and the unperturbed separatrix at $R=2.125$ m. The dotted line marks the position of the "perturbed separatrix".

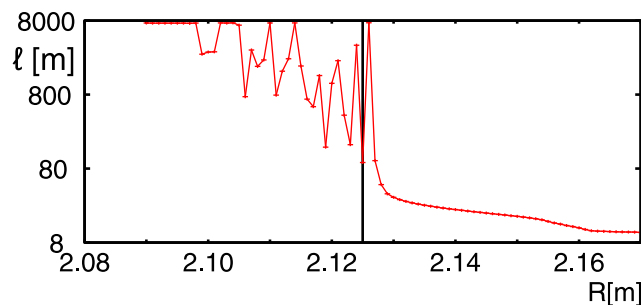


Fig 3: Connection length to the low field side target for field lines starting at the position of the lithium beam diagnostic ($z=0.326$, $\phi=193^\circ$; cut through fig. 2. The position of the unperturbed separatrix is indicated.

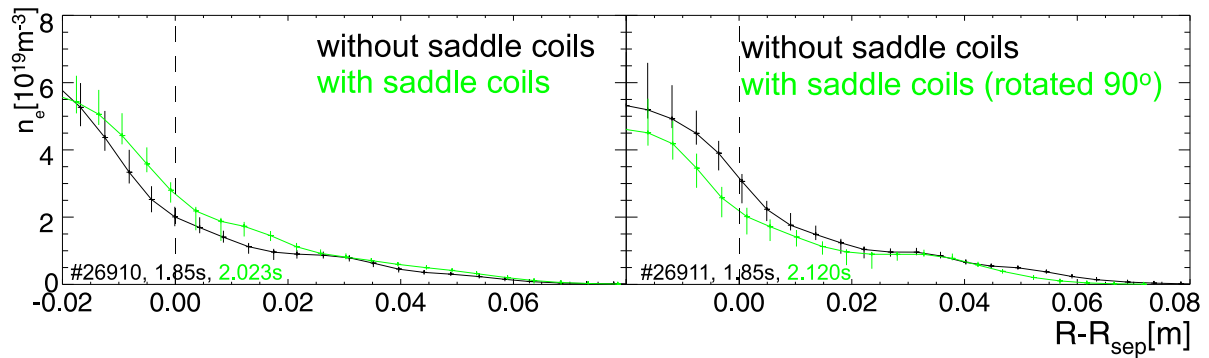


Fig. 4: Density profiles from the lithium beam as a function of the distance to the unperturbed separatrix at the height of the beam at time points between ELMs shortly before (black) and after (green) switching on the saddle coils. The left picture is from the discharge from figures 2 and 3, the right picture for an identical shot where the magnetic perturbation has been rotated by 90°.

around the torus. Figure 3 shows a cut through the values from figure 2 at the position of the lithium beam ($\varphi=193^\circ$). For an ideal, unperturbed equilibrium this connection length would slightly rise in the scrape off layer (SOL) up to the separatrix, where it then jumps to an infinite value. For the perturbed equilibrium we also find the rise in the SOL and a steep increase near the position of the unperturbed separatrix, and finite connection length to the plasma interior indicating the existence of an ergodic zone. (Due to the neglected shielding of the perturbation field by the plasma the width of this ergodic zone is probably over-estimated.) The steep increase of the connection length in the perturbed case can be used to construct a “perturbed separatrix” at the position of the maximum increase, which is indicated in figure 2 as a dotted line. The position of this perturbed separatrix varies sinusoidally around the torus; at the position of the lithium beam it is shifted outwards by about 5mm. This corresponds to a shift in the same direction and magnitude in the density profile measured by the lithium beam diagnostic just before and after the saddle coils have been switched on [4] (figure 4). For an otherwise identical discharge where the configuration of the saddle coils has been rotated by 90° the shift of the perturbed separatrix and correspondingly the shift in the density profile goes in the opposite direction. For the third discharge in this series with even up/down-parity a similar behaviour is observed with a slightly smaller shift of the perturbed separatrix and density profile outwards, and the ergodic zone is smaller than that in the discharges with odd parity.

4. Mapping along flux surfaces

When comparing measurements from different diagnostics, one often assumes constancy along flux surfaces, e.g. for the electron density n_e . However, when using the unperturbed equilibrium to map measurements from different positions onto a common flux coordinate, this may lead to further complications: Figure 5 shows edge density profiles from the Li-beam and Thomson-scattering diagnostics mapped onto the poloidal flux radius ρ_{pol} for the discharge from figures 2 and 3, shortly before and after the saddle coils have been switched

on. Whereas the mapping is quite good without saddle coils, the profiles from the two diagnostics seem to be shifted apart when the coils are switched on. This is mostly due to the fact that the toroidal positions of the two diagnostics differ by 137° and see a different shift of the 'perturbed separatrix', in this case outward for the Li-Beam and inward for the YAG laser of the Thomson scattering diagnostic [5]. Furthermore, when following perturbed field lines around

the torus and comparing to the unperturbed equilibrium, one finds that they cover a certain ρ_{pol} -range and such lead to enlarged error bars in the position when mapping to ρ_{pol} .

5. Strike point splitting

During phases where the saddle coils are switched on, often a splitting of the maximal power density on the target plate recorded by thermographic cameras is observed, which is described as strike point splitting. It seems that the positions of these strike points can partially already be

explained with the simple model where the vacuum field of the saddle coils is added to the unperturbed equilibrium: Figure 6 shows the minimal flux coordinate ρ_{min} (of the unperturbed equilibrium) for field lines ending at the outer target plate at the toroidal position of the thermographic camera. Assuming that field lines with smaller ρ_{min} originate from hotter plasma layers and hence transport more energy to the target plates, the radial ρ_{min} distribution should be correlated with the radial power deposition maxima as confirmed in figure 6 and also seen at JET [6]. However, although this model may describe the positions of these strike points, it cannot explain under which conditions strike point splitting occurs.

References

- [1] W. Suttrop et al., Phys. Rev. Lett. 106 , 225004 (2011) and this conference, I2.109
- [2] P.J. McCarthy et al, Phys. Plasmas 6, 3554-3560 (1999)
- [3] E. Strumberger, E. Schwarz, Report 5/112, Max-Planck-Inst. f. Plasmaphysik (2005)
- [4] R. Fischer et al, this conference P1.072
- [5] B. Kurzan et al, this conference P4.048
- [6] D. Harting et al., submitted to Nuclear Fusion

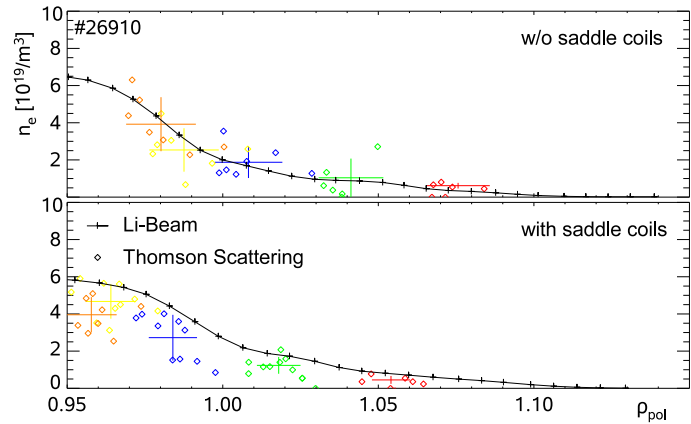


Fig. 5: Mapping of the density measurements from Li-Beam (black) and Thomson-Scattering (colored, each color denotes one channel) on the normalized poloidal flux radius ρ_{pol} for the discharge from figures 2 and 3. Thomson-Scattering measurements are averaged over 100ms, only using time points between ELMs.

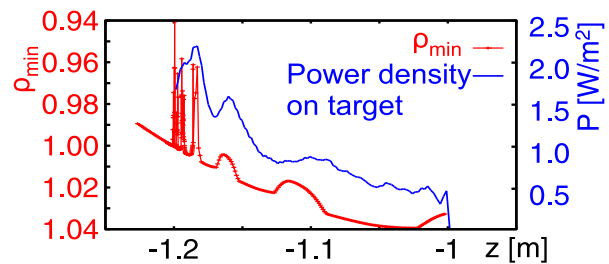


Fig. 6: Power density along the outer target plate (blue) and ρ_{min} for field lines starting at this target (red) during a phase with saddle coils switched on.